Impacts of DC Circuit Breakers on AC/DC System Stability Subject to DC Faults

Gen Li[1], Jun Liang[1], Carlos E Ugalde-Loo[1], Paul Coventry[2]
*1 Institute of Energy and Environment, Cardiff University, Cardiff, UK
*2 National Grid, Warwick Technology Park, Warwick, UK

***Abstract*—In a voltage source converter-based (VSC) multi-terminal high voltage direct current (MTDC) grid, the resistances dominate the impedances of the transmission system. Therefore, the inductances tend to have a small impact on the propagation of a DC fault. Additionally, an AC side connected system will feed current to the fault through anti-parallel diodes, which can be seen as a three-phase fault on the AC side of a converter. This means that all parts of an MTDC grid will be affected if a DC fault cannot be isolated quickly. From the viewpoint of an AC system, a DC fault is thus seen as "multi-point" AC faults. In this paper, the transient characteristics of an AC/DC network using DC circuit breakers (DCCBs) to isolate a DC fault are studied. The influence of different operating times and sizes of DC reactors are considered. For completeness, the power angle and AC voltage stability of the AC connected systems are examined. The input impedance of the VSC is defined to analyse the "multi-point" faults. Simulations are performed using PSCAD/EMTDC, where an integrated AC/DC transmission system is modelled. In addition to providing a further understanding on the dynamic behaviour of AC/DC systems during DC fault conditions, the studies in this paper show that an increase in the operating speed of the DCCBs provides better results to mitigate the impacts of "multi-point" faults than by increasing the size of the DC reactor. A balance between these two aspects may contribute to the risk-managed deployment of DCCBs –which is essential to design effective protection strategies for combined AC/DC systems.**

***Index Terms*—DC circuit breaker, MTDC grid, AC/DC interactions, fault analysis, transient behaviour.**

I. INTRODUCTION

The voltage source converter-based (VSC) high voltage direct current (HVDC) technology has experienced a great development over the last decades due to the following features: 1) compact and flexible station layouts, with low space requirements, and a scalable system design; 2) a high dynamic performance and stable operation with AC networks; 3) supply of passive networks and black-start capability; 4) an independent control of active and reactive power; and 5) STATCOM features [1]-[5].

The first commercial VSC-HVDC project was built in 1997 on the island of Gotland [6]. Since then, the ratings have increased and applications have progressed rapidly. However, most commercial projects are point-to-point HVDC links, except for the 3-terminal Nan'ao project [7] and the 5-terminal Zhoushan project [8] in China. Deployment of multi-terminal high voltage direct current (MTDC) grids could bring advantages over point-to-point links; for instance, MTDC grids could reduce the number of converter stations and transmission circuits for integrating multiple types of sources and loads [9].

An MTDC grid consists of multiple converters and DC links, which provide redundancy and capability for fast fault isolation. However, one of the major obstacles preventing further development is the lack of fast, reliable and low-loss commercial HVDC circuit breakers (DCCBs) [10]-[11]. The absence of cyclic zero current-crossings in a DC system inherently makes DC current switching more difficult than in AC systems, as arcs require a zero-crossing to be extinguished. DCCBs have to interrupt DC fault currents very quickly and need to dissipate the large energy stored in the DC reactors [11]. Although substantial work has been done in DCCBs, the on-state losses and operating speed are still areas where further research effort is required.

Unlike AC systems, resistances dominate the impedance of the transmission circuits within MTDC grids. Since there is no inertia contribution from the converters, MTDC systems can be considered as low-inertia systems. During a DC fault, the DC voltage will drop quickly in all terminals. Although insulated-gate bipolar transistors (IGBTs) will be blocked by the local protection systems of the converters, currents from the AC side will feed to the fault through anti-parallel diodes (except for the case when full-bridge modular multilevel converters, MMCs, are used). This is equivalent to a three-phase short-circuit in the AC side of a converter. Therefore, if a VSC-based MTDC grid interconnects with an AC system at multiple points, a DC fault within the grid can be seen as "multi-point" faults on its connected AC system. These faults will be continuously penetrating the adjacent AC system if the DC fault cannot be isolated in a reliable manner. Attention should be exercised as this may lead to instability of the overlay AC/DC system and, therefore, the transient characteristics of the overall AC/DC system should be investigated in further detail.

In this paper, the AC system voltage and power angle stability of an integrated AC/DC transmission network during a DC fault are studied. DCCBs are employed to interrupt DC fault currents. The input impedance of the VSCs is defined to analyse the impacts of "multi-point" faults on the stability of AC systems. Factors that influence the stability and dynamic performance of the overall AC/DC system, such as the operating time of DCCBs and the size of DC reactors, are

investigated. Simulations are carried out using PSCAD/ EMTDC, with results showing that the impact of increasing the value of the DC reactor to mitigate a "multi-point" fault is less pronounced when compared to increasing the operating speed of DCCBs. The work presented in this paper contributes to a further understanding of the transient behaviour in AC/DC systems when DCCBs are used to isolate DC faults.

II. High Voltage DC Circuit Breakers

At present, there is no commercially available high voltage DCCB, which is one of the major obstacles for large scale deployment of MTDC grids. Technical demands for DCCBs are high. The fault current interruption time must be much shorter than that of an AC circuit breaker (ACCB) due to the lower impedance of the DC transmission lines. Voltage drops caused by a DC fault propagate very quickly; therefore, the fault should be cleared within milliseconds to mitigate its impact on the healthy sections of the MTDC grid. Another difficulty preventing the manufacture of fast DCCBs is the absence of natural zero-crossings in DC currents [10]-[14].

The most common DCCB technologies are shown in Fig. 1 and are discussed in the following subsections.

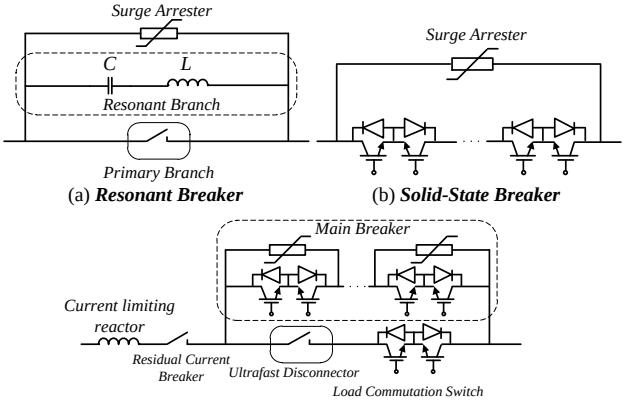

Fig. 1. Types of high voltage DCCBs.

A. Resonant DCCB

Fig. 1(a) illustrates the schematic diagram of a resonant breaker. One of the parallel branches consists of a resonant *LC* circuit, which gives the name to the device. The resonant breaker creates a current zero-crossing suitable for the interruption of the DC fault current [10].

In normal operating condition, current flows through the primary branch, which consists of a low-loss mechanical breaker. The mechanical switch will open once a DC fault is detected and an arc will be created. The fault current will commutate to the resonant circuit where a resonant current will be produced. A zero-crossing will appear in the mechanical switch after some oscillations, but the arc can be interrupted at the first zero-crossing [10]-[11]. Although the costs and on-state losses of this DCCB are low, the operating time is significant slower than its counterparts.

B. Solid-State DCCB

The solid-state breaker (Fig. 1(b)) is based on fully controlled semiconductor switches (*e.g.* IGBTs). It can operate very quickly, with a switching time of a few microseconds [10]. Its drawbacks are the high costs of power electronic devices and the high on-state losses.

C. Hybrid HVDC Breaker

This is shown in Fig. 1(c). It is based on fast mechanical switches and power electronics switches and combines the merits of the resonant and solid-state breakers [11]-[14]. The low-loss branch consists of an ultrafast disconnector and a load commutation switch. In the main breaker, IGBTs are connected in series and a surge arrester is used to exhaust the fault current.

During normal operation, current flows through the low-loss branch and the main breaker is blocked. If a DC fault is detected, the load commutation switch will be blocked and the main breaker will be fired simultaneously. The fault current then commutates into the main breaker. Once the current in the low-loss branch becomes zero, the ultrafast disconnector opens with a quite low voltage stress. Then the main breaker is blocked to commutate the fault current into the arresters, where the energy stored in the DC reactors is absorbed [13].

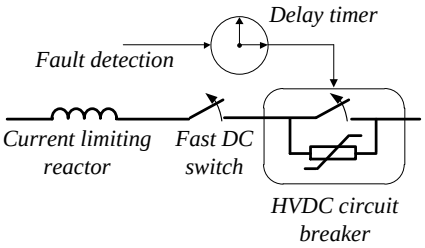

Fig. 2. A reduced DCCB model for simulation.

In this paper, it is assumed that the internal design of the DCCBs does not influence the system dynamic response. Therefore, a reduced DCCB has been modelled as an ideal breaker with a surge arrester (shown in Fig. 2). A fast DC switch and a current limiting reactor are equipped with the DCCB. A delay timer is set to simulate the time for fault discrimination and fault-location. This model is able to emulate a hybrid DCCB during several milliseconds or a mechanical DCCB during tens of milliseconds [9].

III. Methodology and Test System Modelling

A. Methodology

If a short-circuit occurs in an AC system, the voltage will drop and current will increase at the fault location. The impedance at this point will decrease near to zero. However, other places in the AC system far from the fault may not be affected by this impedance change. The distance protection method is based on this principle, which considers the ratio of measured voltages to measured currents [15].

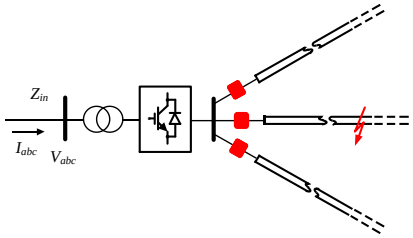

Fig. 3. Measurements of the input impedance of a VSC.

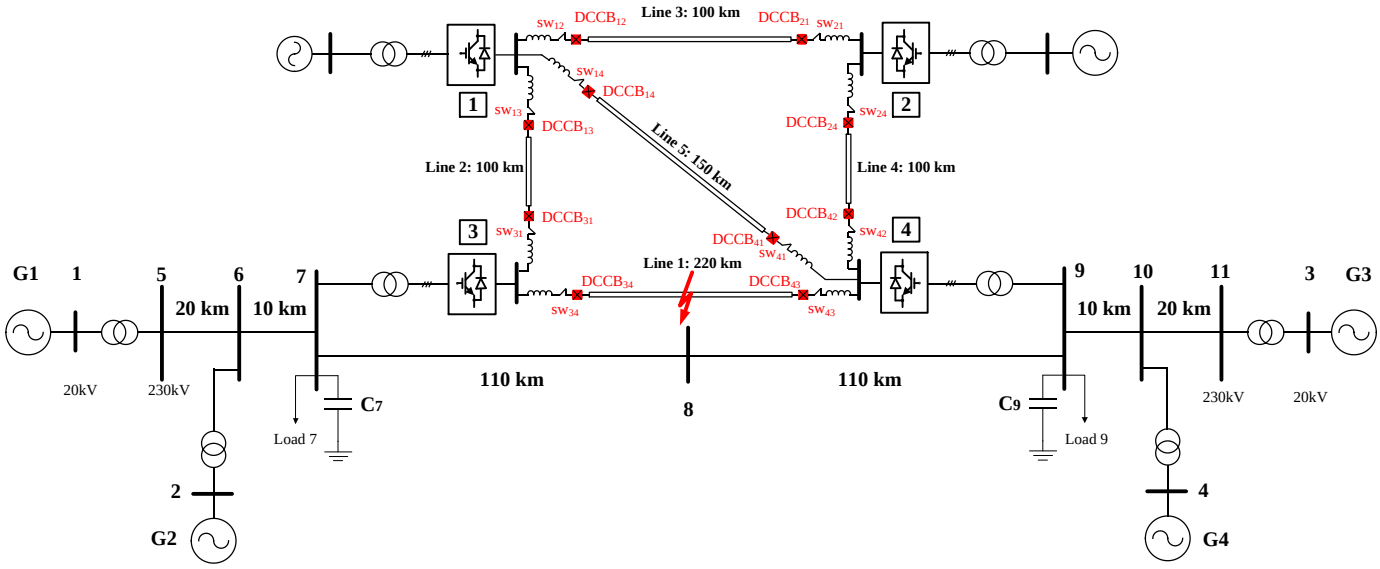

Fig. 4. Integrated AC/DC transmission test system with DCCBs.

In order to show that a DC fault in an MTDC grid can be seen as "multi-point" faults by its connected AC system, the concept of impedance measurement is borrowed from distance relaying in AC systems. The input impedance of a VSC during a DC fault is defined as the equivalent impedance as seen from the AC side of a converter into the DC system.

The concept of input impedance (Z_{in}) is illustrated in Fig. 3. As it can be seen, currents and voltages are measured at the AC side of a converter. Equations (1)-(3) are used to calculate the magnitude of Z_{in} :

$$V_{rms} = \sqrt{\frac{V_a^2 + V_b^2 + V_c^2}{3}} \quad (1)$$

$$I_{rms} = \sqrt{\frac{I_a^2 + I_b^2 + I_c^2}{3}} \quad (2)$$

$$Z_{in} = \frac{V_{rms}}{I_{rms}} \quad (3)$$

The input impedance can be used to describe the electrical distances within an MTDC grid during a DC fault. If the value of Z_{in} of different converters drops to a similar value, this implies that the DC fault is equivalent to "multi-point" faults from the viewpoint of the connected AC system.

The studies presented in this paper focus on the impact that DC faults have on AC system stability. To achieve this, the phase angles of synchronous generators and AC bus voltages in the AC system are used. Different DCCB operating times and values of the DC reactor will be examined to investigate the effect on the value of Z_{in}.

B. *Test System Modelling*

An integrated AC/DC power transmission system, shown in Fig. 4, has been developed in PSCAD/EMTDC. The system consists of the four-machine two-area AC system reported in [15] which has been upgraded to include a four-terminal meshed HVDC grid.

The MTDC grid can represent offshore DC systems connecting offshore wind farms to onshore AC grids. Every DC cable has a DCCB at each end. Converters 1 and 2 are connected to equivalent AC systems (which are not of special interest in this investigation). Converters 3 and 4 are connected to buses 7 and 9 of the AC system. Each synchronous generator is modelled together with an exciter, a turbine and a governor. The converters are two-level VSCs with a symmetrical monopole configuration.

Although half-bridge MMCs are now widely adopted, a two-level VSC has a very similar DC fault behaviour [16]. As it will provide a reasonably similar impact on the connected AC systems it is thus adopted in this work. The parameters of the DC grid are given in Table I. The data for HVDC cables has been taken from [17]. The cable lengths are indicated in Fig. 4.

TABLE I. PARAMETERS OF THE TEST SYSTEM

Parameter	Value
Rated Converter Power (Monopole)	900 MW
DC voltage	± 320 kV
AC side voltage (L-L,RMS)	230 kV
Transformer ratio	230/400kV
AC system frequency	50 Hz
Transformer Leakage Reactance	0.1 p.u.
Converter Phase Reactor L_s	0.05 p.u.
DC Capacitor C_{cap}	200 μF
Current limiting inductor L_r	100 mH

IV. SIMULATION RESULTS AND ANALYSIS

The IGBTs from the converters cannot withstand large fault currents; therefore, the converter internal protection systems will block the IGBTs to prevent damage.

The converter local protection is based on an overcurrent and rate-of-rise of current criterion. Once the rate-of-rise of the current flowing through the converter is higher than 3 kA/ms or if the current exceeds twice the value of rated DC current, tripping signals will be sent to block the IGBTs. The converter local protection logic is shown in Fig. 5.

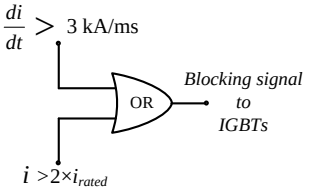

Fig. 5. Logic of converter local protection.

To investigate the worst fault scenario, a solid pole-to-pole fault has been applied at t = 6 s in the middle of Line 1 for each simulation study. A fault resistance of 1 Ω is considered. The current flowing through $DCCB_{34}$, the DC voltages of each converter, the voltages of AC buses 7 and 9, the power angle difference between generators 1 and 3 and the power transferred in the AC corridor will be measured and analysed. Different DCCB operating times and different DC reactor values are considered to study the input impedance of VSCs.

It should be emphasised that a detailed fault isolation and post-fault restoration algorithm falls out of the scope of this paper and thus no further discussion is warranted.

A. Influence of DCCB Operating Times

Simulations are performed to assess the effect of different DCCB operating times, with results shown in Fig. 6. $DCCB_{34}$ and $DCCB_{43}$ trip at 5, 20 and 60 ms. As it can be seen, a decrease in the operating times enables a faster system recovery to steady state. When the DCCBs operate 60 ms after the fault (for instance, due to a long decision making algorithm time or to the use of mechanical DCCBs), the phase angle between synchronous generators 1 and 3 experiences large oscillations, which means that the AC system is severely impacted.

It can be observed that the AC voltages of both buses are affected at almost the same time. When the DCCBs trip 5 ms after the fault, the system will recover to steady state, leading to a voltage increase in bus 7 and a voltage decrease in bus 9.

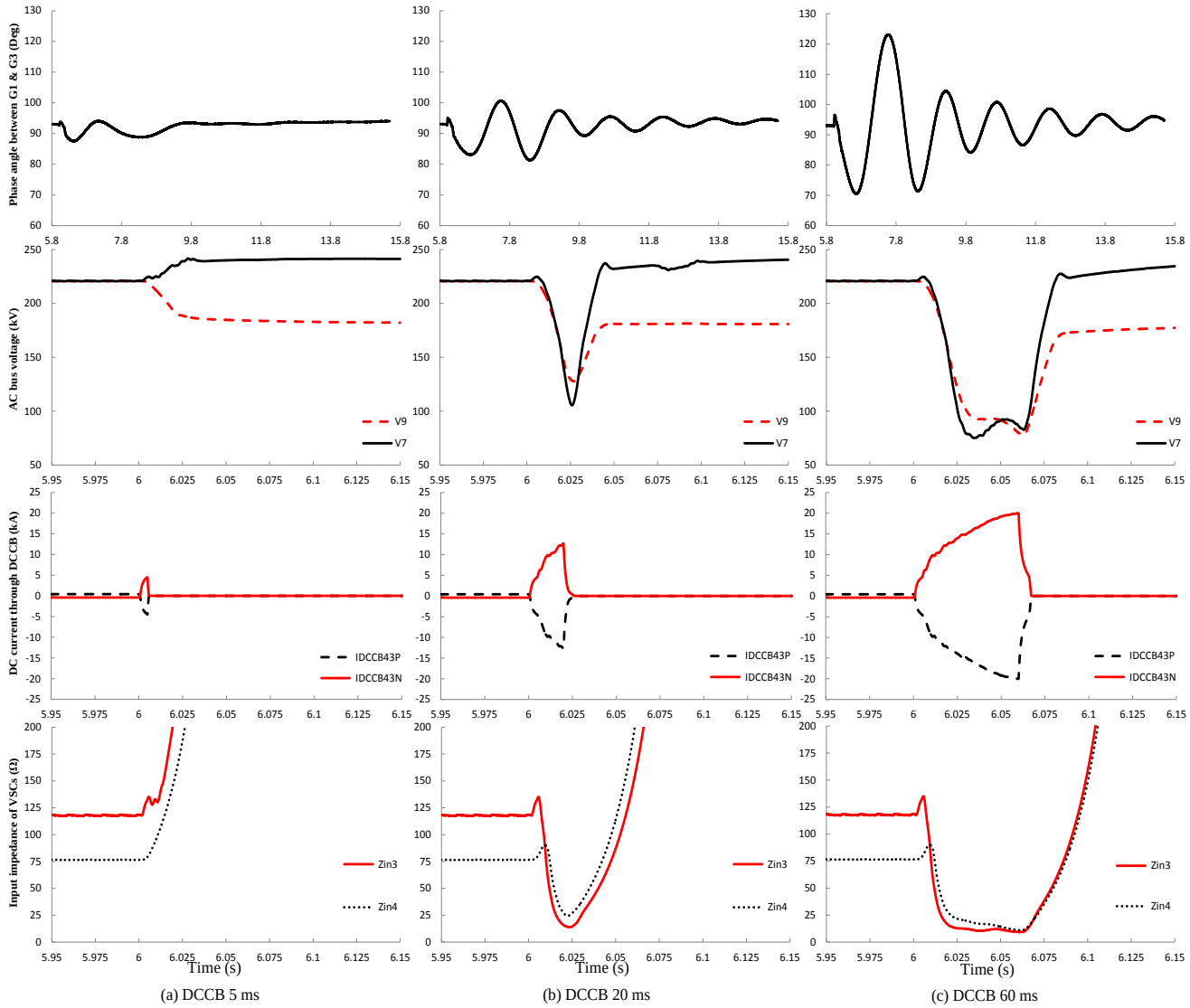

(a) DCCB 5 ms (b) DCCB 20 ms (c) DCCB 60 ms

Fig. 6. System responses during a DC fault with different DCCBs operating time.

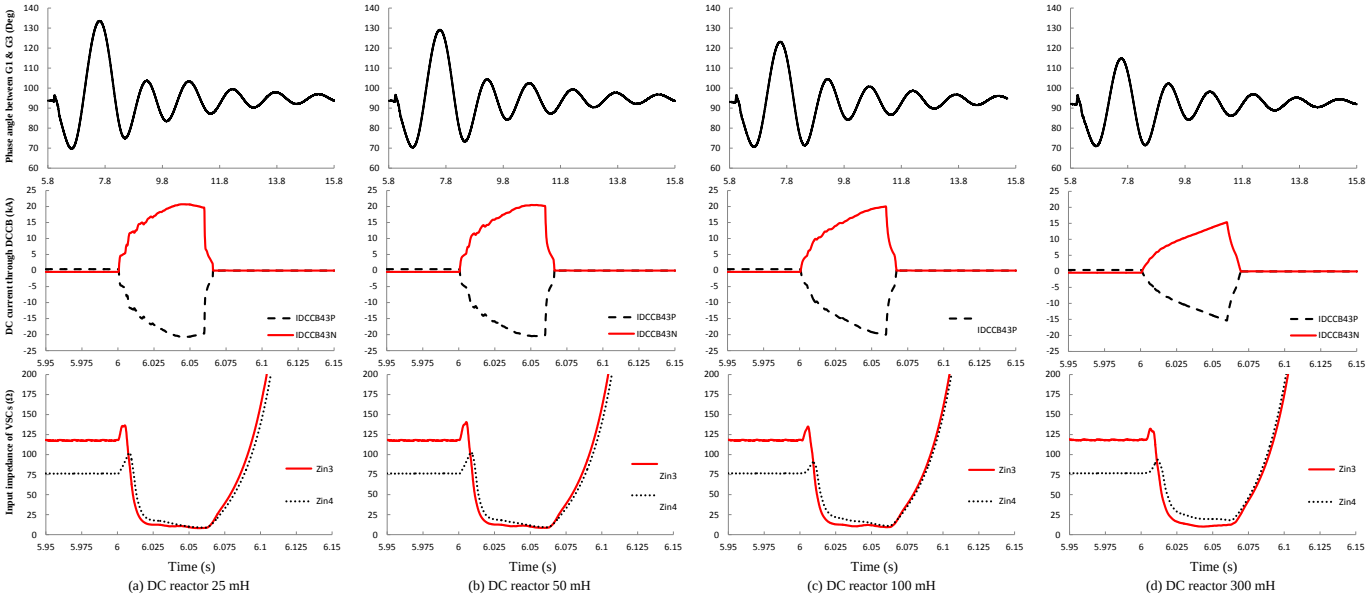

(a) DC reactor 25 mH (b) DC reactor 50 mH (c) DC reactor 100 mH (d) DC reactor 300 mH

Fig.7. System responses during a DC fault with different values of DC reactors.

If the DC fault is not isolated quickly, the DC voltage will continue to drop and AC currents will start to feed into the DC side once the DC voltage is lower than the AC line-to-line voltages. Following this, AC voltages will drop considerably.

As it can be seen in Fig. 6(c), the DC fault current increases to more than 20 kA when a 60 ms operating time is employed. This value goes beyond the current interrupting capabilities of any available DCCB. In practical applications, a DC reactor would be used to limit the rate-of-rise of fault current so that the DCCBs can interrupt the fault within its rated current.

Fig. 6 also shows the input impedance Z_{in} of converters 3 and 4. During normal operation, Z_{in3} and Z_{in4} have different values since each converter has different set points. However, both drop quickly and reach a similar value if the DC fault is not isolated fast enough. As discussed previously, this implies that the fault in the MTDC grid could be interpreted as "multi-point" faults in the adjacent AC system. In this case, the stability of the overall system may have been compromised. It should be highlighted that the input impedances cannot become zero due to the impedance contribution of the AC transformer, AC and DC reactors and DC cables.

B. Influence of DC Reactors

The influence that the size of a DC reactor has on the input impedance of the VSC is studied in this section. In order to investigate the worst case scenario, the DCCB operating time has been set to 60 ms, which provided the poorest responses in the simulations of Section IV-A. The values employed for the DC reactor are shown in the captions of Fig. 7.

Results in Fig. 7 illustrate that a large DC reactor can limit the rate-of-rise of DC fault current significantly and therefore reduce the current interruption duty of DCCBs. However, it should be emphasised that the DC reactor size does not influence the magnitude of the steady state fault current [17]. Therefore, a change in the DC reactor size will not modify the magnitude of the input impedance considerably. In other words, the DC fault still behaves as "multi-point" faults on its connected AC system.

Based on the results obtained in the previous simulations, an increase in the operating speed of DCCBs provides better results to mitigate the impact of "multi-point" faults than an increase in the size of the DC reactor. However, it should be highlighted that the inclusion of a large reactor may increase the time constant of the system; this in turn may affect the system dynamic response and, in the worst case, may cause instability. The design of DCCBs should be thus assessed comprehensively both at device and at system levels.

V. CONCLUSIONS

In this paper, the effects that DCCBs have on AC/DC system stability following DC faults have been analysed and assessed. Studies have been carried out using different DCCB operating times and considering different sizes for the DC reactor of the DCCBs. The input impedance as seen from the AC side of the VSCs has been defined. Simulations have been performed using an AC/DC system modelled in PSCAD/EMTDC.

The studies show that the magnitude of the input impedances in the integrated AC/DC system move towards a similar value during a DC fault. This implies that a DC fault can be seen as "multi-point" faults on its connected AC system. This occurs as the electrical distances of the connecting points of the AC/DC system are shortened during the fault. As a consequence, voltage and power angle instability will result if the fault is not isolated quickly.

The combination of DCCBs with DC reactors can provide fast DC fault clearance, thus preventing that a large steady state current is reached. However, an increase in the size of the DC reactor to mitigate "multi-point" faults provides limited benefits when compared to faster operating speeds of the DCCBs. Therefore, fast and reliable high voltage DCCBs are essential to build robust integrated AC/DC grids.

APPENDIX

MTDC System Operating Data: This is given in Table II.

TABLE II.

CONTROL PARAMETERS FOR THE STEADY-STATE CONTROL STRATEGY

Converter	**Control Parameters**
VSC 1	V_{dcref1} = ± 320 kV; Q_{ref1} = 40 MVAr
VSC 2	P_{ref2} = –300 MW; Q_{ref2} = –30 MVAr
VSC 3	P_{ref3} = 400 MW; Q_{ref3} = 40 MVAr
VSC 4	P_{ref4} = –600 MW; Q_{ref4} = –120 MVAr

* The active and reactive power flows from the AC system into each converter are positive.

Loads and Compensated Reactive Power: The loads and reactive power supplied by the shunt capacitors at buses 7 and 9 are provided in Table III.

TABLE III. LOADS AND COMPENSATED REACTIVE POWER

	Active power	Reactive power	Compensated reactive power
Bus 7	1000 MW	100 MVAr	350 MVAr
Bus 9	2700 MW	250 MVAr	400 MVAr

ACKNOWLEDGEMENTS

The research leading to these results has received funding from the People Programme (Marie Curie Actions) of the European Union's Seventh Framework Programme FP7/2007-2013/ under REA grant agreement no. 317221, project title MEDOW, and from the National Grid project TAO/22434, UK

REFERENCES

[1] J. Liang, T. J. Jing, O. Gomis, J.B. Ekanayake, N. Jenkins, "Operation and Control of Multiterminal HVDC Transmission for Offshore Wind Farms," *IEEE Transactions on Power Delivery*, vol. 26, no.4, pp. 2596-2604, Oct. 2011.

[2] X. Hu, J. Liang, D. J. Rogers and Y. Li, "Power Flow and Power Reduction Control Using Variable Frequency of Offshore AC Grids," *IEEE Transactions on Power Systems*, vol. 28, no. 4, pp. 3897-3905, Nov. 2013.

[3] D. van Hertem, O. Gomis, J. Liang, *HVDC Grids: For Offshore and Supergrid of the Future*, Wiley-IEEE Press, 2016.

[4] S. Debnath, J. Qin, B. Bahrani, M. Saeedifard and P. Barbosa, "Operation, Control, and Applications of the Modular Multilevel Converter: A Review," *IEEE Transactions on Power Electronics*, vol. 30, no. 1, pp. 37-53, Jan. 2015.

[5] J. Liang, O. Gomis-Bellmunt, J. Ekanayake and N. Jenkins, "Control of multi-terminal VSC-HVDC transmission for offshore wind power," in *13th European Conference on Power Electronics and Applications EPE '09*, Barcelona, Spain, 2009, pp. 1-10.

[6] ABB HVDC Light, Gotland HVDC Light, [Online]. Available: http://new.abb.com/systems/hvdc/references/gotland-hvdc-light.

[7] R. Hong, "Architecture of Nan'ao multi-terminal VSC-HVDC system and its multi-functional control," *CSEE Journal of Power and Energy Systems*, vol. 1, no.1, pp. 9-18, March 2015.

[8] G. F. Tang, Z. Y. He, H. Pang, X. M. Huang and X. P. Zhang, "Basic topology and key devices of the five-terminal DC grid, " *CSEE Journal of Power and Energy Systems*, vol. 1, no. 2, pp.22-35, June 2015.

[9] G. Li, J. Liang, C. E. Ugalde-Loo, P. Coventry and J. Rimez, "Dynamic interactions of DC and AC grids subject to DC faults," in *IEEE 8th International Power Electronics and Motion Control Conference (IPEMC-ECCE Asia)*, Hefei, China, 2016, pp. 2627-2633.

[10] K. Tahata, S. El Oukaili, K. Kamei, D. Yoshida, Y. Kono, R. Yamamoto and H. Ito, "HVDC circuit breakers for HVDC grid applications," in *11th IET International Conference on AC and DC Power Transmission*, Birmingham, U.K., 2015, pp. 1-9.

[11] M. Hajian, D. Jovcic and B. Wu, "Evaluation of Semiconductor Based Methods for Fault Isolation on High Voltage DC Grids," *IEEE Transactions on Smart Grid*, vol. 4, no. 2, pp.1171-1179, June 2013.

[12] M. Callavik, A. Blomberg, J. Hafner and B. Jacobson, "The hybrid HVDC breaker: An innovation breakthrough enabling reliable HVDC grids", ABB Grid Systems, Technical Paper, Nov. 2012.

[13] R. Derakhshanfar, T.U. Jonsson, U. Steiger and M. Habert, "Hybrid HVDC breaker – Technology and applications in point-to-point connections and DC grids," in *CIGRE Session*, Paris, France, 2014, pp. 1-11.

[14] C. D. Barker, R. S. Whitehouse, A. G. Adamczyk and M. Boden, "Designing fault tolerant HVDC networks with a limited need for HVDC circuit breaker operation", in *CIGRE Session*, Paris, France, 2014.

[15] P. Kundur, *Power System Stability and Control*, EPRI Power System Engineering Series. New York: McGraw-Hill, 1994, p.904.

[16] M. Hajian, L. Zhang and D. Jovcic, "DC Transmission Grid With Low-Speed Protection Using Mechanical DC Circuit Breakers," in *IEEE Transactions on Power Delivery*, vol. 30, no. 3, pp. 1383-1391, June 2015.

[17] M. K. Bucher and C. M. Franck, "Contribution of Fault Current Sources in Multiterminal HVDC Cable Networks," *IEEE Transactions on Power Delivery*, vol. 28, no. 3, pp. 1796-1803, July 2013.

CONTACT INFORMATION

Gen Li is with the Institute of Energy and Environment, Cardiff University, Cardiff, UK, CF24 3AA (phone number: +447404608844, e-mail: lig9@cardiff.ac.uk).